Evolution of caves in porous limestone by mixing corrosion: A model approach

Wolfgang Dreybrodt[1], Douchko Romanov[2] and Georg Kaufmann[2]

[1]Karst Processes Research Group, Institute of Experimental Physics, University of Bremen, 28359 Bremen, Germany; (dreybrodt@ifp.uni-bremen.de)

[2]Institute of Geological Sciences, FU Berlin, Malteserstr. 74-100, Building D, 12249 Berlin, Germany; (dromanov@zedat.fu-berlin.de, gkaufma@zedat.fu-berlin.de)

Geologia Croatica

ABSTRACT

When water from the surface, e.g. from a lake, flows down through porous carbonate rocks, through a region with high hydraulic conductivity and encounters the water table of a phreatic aquifer, both waters mix by diffusion along their boundary. In a carbonate aquifer, where both surface and phreatic waters are saturated with respect to calcite, mixing corrosion causes renewed dissolution capacity Δc_{eq} of the carbonate rock in the diffusion-mixing zone, extending from the boundary separating the phreatic water from the surface water encountering it. A numerical model is presented from which the initial change of porosity in such a diffusion-mixing zone is obtained. The initial change of porosity can be calculated from the local distribution of the mixing ratio, and the second derivative of Δc_{eq} with respect to m. $m(x,y)$ is the spatial distribution of the mixing ratio $m= V_{surf}/(V_{suf}+ V_{prh})$, where the V's assign the corresponding volumes of surface and phreatic water. The second derivative has been calculated for three geochemical scenarios with differing CO_2-concentrations of surface and phreatic water by the use of PHREEQC-2. The spatial distribution $m(x,y)$ is obtained by using MODFLOW and MT3DMS in a modelling domain with constant hydraulic conductivity for various flow velocities of the phreatic aquifer. The time scale of cave evolution is estimated from the results. Passages of dimensions of about one metre in width and several 10 cm in height, extending in length along the boundary line, where surface and phreatic waters meet, can be created in time scales of 10 000 years. These caves are horizontal with blind ending passages and closely resemble the isolated caves observed in Central West Florida.

Keywords: speleogenesis, porous limestone, mixing corrosion, caves, Florida

1. INTRODUCTION

Caves in young porous rocks are remarkably different from those in ancient fractured rocks. In the latter, speleogenesis is governed by flow along fractures, such as bedding planes and joints, and the matrix conductivity is negligible. Consequently, conduits develop along the flow directions in these fractures and their walls are solid rock without any porosity. The speleogenesis of these caves was the focus of research for two decades (DREYBRODT et al., 2005; DREYBRODT & GABROVSEK, 2003; PALMER, 1991; PALMER, 2007; FORD & WILLIAMS, 2007; KAUFMANN, 2005).

Caves in porous rocks, however, where the flow is not guided along fissures but where water is transported by Darcy flow through the matrix of the rock are different. They are known from young carbonate islands. Here mixing of saltwater with freshwater creates flank margin caves along

the rim of the island. These isolated caves at the freshwater lens, originate as chambers of moderate size without entrances and exits, MYLROIE & CAREW, (1990, 2000, 2003), ROMANOV & DREYBRODT (2006), DREYBRODT & ROMANOV (2007).

In the porous rocks of Central West Florida, isolated caves are also common. FLOREA (2006), FLOREA & VACHER (2004), and FLOREA et al. (2007) have described caves of moderate passage length with blind ending passages. Most of these are aligned along NW–SE and NE–SW regional discontinuities as revealed from photo lineament features on the surface. The cave passages are not longer than several hundred metres and do not represent an integrated system of passages between inputs and outputs of the aquifer. The walls of these caves consist of porous rock with many small-scale solution features. The principal horizons of cave development appear between 3 m and 5 m; 12 m to

Figure 1: a) Geometry of the hydrological concept: Water from a lake at the surface flows along some discontinuity with high hydraulic conductivity, down to the water table of an unconfined aquifer. The surface water encounters this water table along the z-axis and floats with some depth on the phreatic water along the streamline (DS), dividing the two domains of water. Both waters are saturated with respect to calcite, but have differing CO_2 concentrations. A diffusion-mixing zone is created along the dividing streamline (DS) of both water bodies. Therefore mixing corrosion becomes active creating porosity along the z-axis close to the dividing streamlines. The small rectangle close to the origin of the coordinate system represents the region where the modelling domain is located. b) Close up view of a transect showing the rectangle in the x–y plane of Fig.1a. Due to the infiltration, a mound of surface water builds up. Its upper boundary creates the new water table. Its lower border is the dividing streamline (DS) separating phreatic water from surface water. Black triangles indicate the flow directions. The rectangle MD represents the modelling domain, shown in Fig.2.

15 m; and 20 m to 22 m above present sea level. These horizons of cave development are related to prior phreatic water tables (FLOREA, 2006; FLOREA et al., 2007) of an unconfined aquifer. The caves originate from the following speleogenetic processes. When water from the surface above, e.g. a lake, reaches such a water table, it is already saturated with respect to calcite. It is mixed with the phreatic water, also in equilibrium with respect to calcite. When the CO_2 concentrations of both waters differ, mixing corrosion boosts the dissolution capacity (DREYBRODT, 1988). Due to the low hydraulic gradients and the slow flow velocity v_y, between 10^{-7} to 10^{-6} m/s, (HANSHAW et al., 1965; DAVIS, 1996) the mixed solution again becomes saturated after several tens of centimetres. Therefore initial changes of porosity are restricted to a region close to the boundary line where surface water and phreatic water meet and voids directed vertical to the flow of the phreatic water originate.

Since both bodies of water exhibit Darcy flow, mixing of the phreatic water with the surface water can only be affected by molecular diffusion and transversal dispersion across the dividing streamline (DS). The diffusion-mixing zone between surface water and the phreatic water zone extends along the z-axis where the surface water enters. Mixing corrosion is active in this region and causes increasing porosity along the z-axis where the surface water enters, and down the y-direction along the dividing streamline. This way an isolated cave passage could originate, similar to those passages observed in porous rocks in Florida. The conduits are orientated normal to the flow direction of water, which has created them. This is similar to the concept of transverse speleogenesis as first suggested by KLIMCHOUK (2007), although flow is through the matrix of the rock and horizontal, parallel to the water table in contrast to the flow ascending through fractures from below in Klimchouk's concept. Here, we will investigate how and over what time scale, caves can originate in such a hydrological setup.

2. THEORETICAL BACKGROUND

Figure 1 represents the geometry of the two domains of phreatic and surface water. It assumes a local input of water from a lake or a river, much larger than the input by meteoric precipitation, which therefore is neglected. Such geological settings are reported in lakes in the Central Lake District, Florida, USA, where huge amounts (up to 4 m/year) of water leak down vertically through the bottom of the lake to the water table of the Upper Floridan Aquifer (MOTZ, 1998; MOTZ et al. 2001). The domain of surface water in Fig. 1 is idealized and can have other shapes. In any case some kind of a new water table will originate above the former water table of the phreatic aquifer. In this mound of water, flow is phreatic and governed by Darcy's law. Because in Darcy-flow, flow lines can never cross, they must become parallel at the boundary between the water of the underlying aquifer and the surface water or in other words along the dividing streamline.

This can be described in the modelling domain shown in Fig. 2. The left hand side input boundary idealizes the first
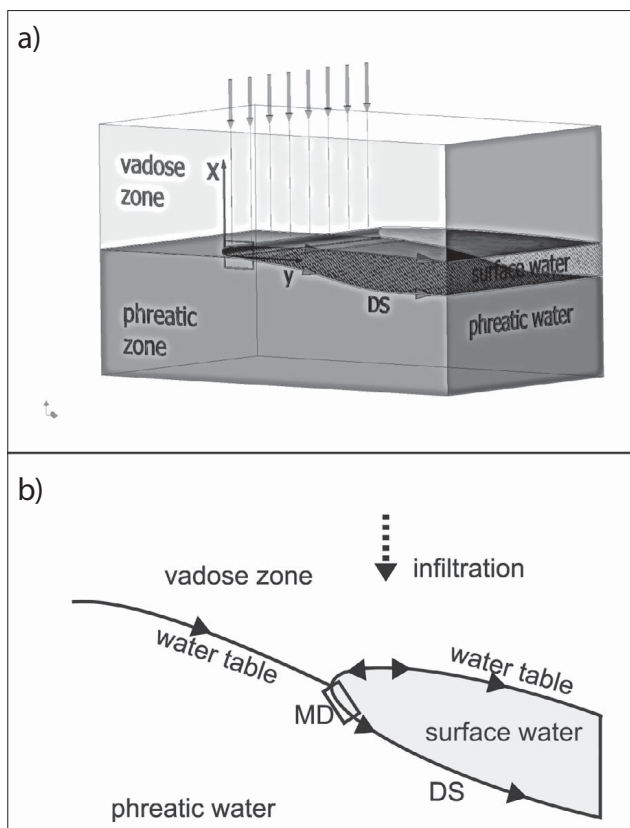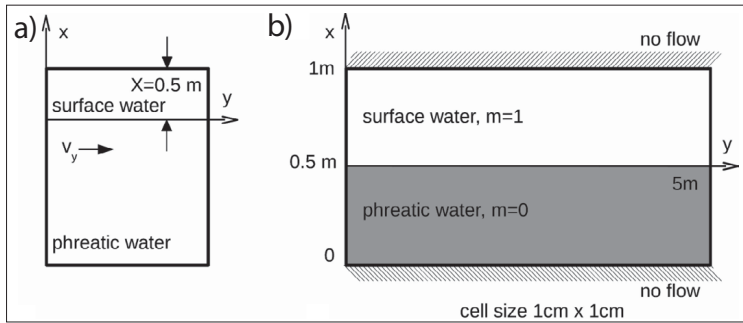
Figure 2: Modelling domain derived from Fig. 1. A constant flow with velocity v_y is injected into the left hand side boundary. For $0 < x < 0.5$m the inflowing water stems from the phreatic aquifer, corresponding to a mixing ratio $m = 0$, whereas the region from 0.5m $< x < 1$m carries water from the surface, with mixing ratio $m = 1$. The right hand side boundary is open for the outflow. The upper and lower boundaries are regarded as impermeable (see text).

encounter of the two water bodies. The y-axis represents the initial part of the dividing streamline. Although the velocities could vary locally, in a first approach we assume a constant flow velocity v_y everywhere in the domain. The corresponding boundary condition is a constant flow rate distributed evenly to all cells of the input boundary. The upper and lower boundaries are impermeable to the transport of dissolved ions. This is true in nature only for the upper boundary representing the new water table. The lower boundary in nature is permeable, because the aquifer reaches much deeper. This, however, is only relevant when the width of the diffusion-mixing zone becomes close to the width of the modelling domain. Therefore care has to be taken that this does not happen in the model calculations. Choosing the width of 1m warrants this. We use cell sizes of 1cm by 1cm. A sharp boundary exists at $x = 0.5$m, $y = 0$ m, with calcium concentrations c_{eq}^{phr} for $x < 0.5$m and c_{eq}^{sur} for $x > 0.5$m. This sharp boundary cannot be maintained downstream or $y > 0$m, because there is transversal diffusion and dispersion causing mixing of the two fluids when they flow down the aquifer. When a parcel of water moves downstream along the y-axis and arrives at the position $v_y \cdot t = y$ after time t, the sharp boundary has been widened to a mixed fringe with width $W_x = 2(D \cdot t)^{1/2}$ in the x-direction, where $D = D_m + v_y \cdot D_m$ is, the transverse dispersion coefficient resulting from molecular diffusion with coefficient D_m and transversal mechanical dispersion by flow with velocity v_y through the pores with diameter d.

This mixing produces undersaturation with respect to calcite and consequently dissolution of carbonate rock. The concentration c_{mix} of the fresh mixed solution depends on the degree of mixing m, which can be written as:

$$c_{mix}(m) = m \cdot c_{eq}^{sur} + (1-m) \cdot c_{eq}^{phr} \qquad (1)$$

with $m = V_{sur}/(V_{sur} + V_{phr})$, where V_{phr} and V_{sur} are the volumes of phreatic and surface water respectively. Due to the renewed aggressivity of the mixed water, its equilibrium concentration with respect to calcite increases by Δc_{eq}. The equilibrium concentration of such mixed water can be written as

$$c_{eq}^{mix}(m) = c_{mix}(m) + \Delta c_{eq}(m) \qquad (2)$$

It can be calculated by use of PHREEQC (PARKHURST & APPELLO, 1999) as a function of m. Since the groundwater velocities are so slow, the mixed solution has sufficient time to come to the new equilibrium, and we can assume that this is true everywhere in the diffusion-mixing zone.

Reactive transport in such a geochemical situation is described by the dispersion-advection-reaction equations of the species involved, which are Ca^{2+} and CO_2. These equations read (DREYBRODT & ROMANOV, 2007; PHILLIPS, 1991)

$$-\Phi \frac{\partial c_i}{\partial t} - \vec{q}\vec{\nabla} c_i + \Phi D(\vec{\nabla} \cdot \vec{\nabla}) c_i = Q_i \qquad (3)$$

where Φ is the porosity of the rock, D is the constant of dispersion, c_i the concentration of species i, $\vec{q}$ the Darcy – flow rate and Q_i the source term of dissolved material. In the limit of fast dissolution ensuring equilibrium of Ca^{2+} with respect to calcite one gets

$$-\Phi \frac{\partial c_{eq}^{mix}(m)}{\partial t} - \vec{q}\vec{\nabla} c_{eq}^{mix}(m) + \Phi D(\vec{\nabla} \cdot \vec{\nabla}) c_{eq}^{mix}(m) = Q_{ceq} \qquad (4)$$

$c_{eq}^{mix}(m,(x,y))$, the equilibrium concentration of calcium with respect to calcite is a function of the mixing ratio m.

The local distribution of m can be represented by the distribution of a non-reactive tracer with a concentration between 1 and 0. Therefore it can be described by a dispersion-advection equation without a source term

$$-\Phi \frac{\partial m}{\partial t} - \vec{q}\vec{\nabla} m + \Phi D\left((\vec{\nabla} \cdot \vec{\nabla}) m\right) = 0 \qquad (5)$$

From equations 4 and 5 Q_{ceq} and from this the resulting change in porosity $d\Phi/dt$ in 1/s [volume (m³) of dissolved rock per (m³/s) of the aquifer] can then be calculated by a simple relation (PHILLIPS, 1991; ROMANOV & DREYBRODT, 2006).

$$\frac{d\Phi}{dt} = -\Phi D \frac{d^2 c_{mix}^{eq}(m)}{dm^2} \left(\vec{\nabla}(m)\right)^2 \frac{M}{\rho} \qquad (6)$$

M is the molar weight of $CaCO_3$ and ρ its density. $m(x,y)$ is the local distribution of mixing in the aquifer. Therefore it is only necessary to solve the diffusion – advection equation (6) for mixing in the aquifer. From Eq.2 one has $d^2 c_{eq}^{mix}/dm^2 = d^2\Delta c_{eq}/dm^2$. This purely geochemical entity is the second derivative of $\Delta c_{eq}(m)$ with respect to m, which can be obtained by use of PHREEQC as shown in Fig. 3b. To obtain $d\Phi/dt$ one has to know the mixing ratio $m(x,y)$ and $d^2\Delta c_{eq}/dm^2$ as a function of the local coordinates. This method has been successfully applied to the evolution of flank – margin caves in the saltwater – freshwater diffusion-mixing zone of coastal carbonate aquifers (ROMANOV & DREYBRODT, 2006).
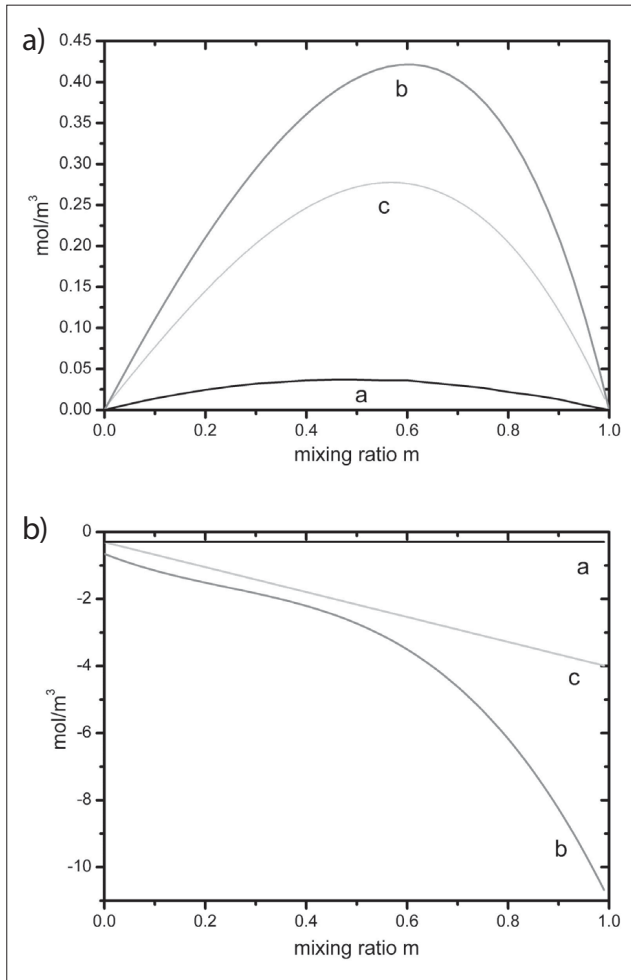
Figure 3: a) Renewed solution capacity Δc_{eq} for surface and phreatic water as a function of the mixing ratio m for three geochemical scenarios. a) (inorganic) P_{CO2} of phreatic water 0.001 atm, P_{CO2} of surface water water 0.01 atm, b) (decay of organic matter). P_{CO2} of phreatic water 0.001 atm, P_{CO2} of surface water water 0.1 atm, c) (decay of organic matter). P_{CO2} of phreatic water 0.0003 atm, P_{CO2} of surface water 0.1 atm. b) second derivatives $d^2\Delta c_{eq}/dm^2$ for the three scenarios a), b) and c).

In the next step we have to find $d^2\Delta c_{eq}/dm$ for realistic geochemical scenarios. Ground waters in carbonate rocks are calcium-bicarbonate dominated. Therefore in a good approximation, for simplicity we assume both waters are pure calcium-bicarbonate waters in the system $CaCO_3$-CO_2–H_2O, saturated with respect to calcite and in equilibrium with some low P_{CO2} – value characteristic for the phreatic water, and with a P_{CO2} – value significantly higher for the water entering from the surface. With these conditions, both waters are completely defined and the chemistry of solutions mixed from these waters can be calculated by geochemical codes such as PHREEQC. We have investigated three different geochemical scenarios. In the first scenario a) we assume $P_{CO2} = 10^{-3}$ atm for the phreatic water and 10^{-2} atm for the water from the surface. This is a case dominated by an inorganic chemistry. Fig. 3a shows the results of PHREEQC at a temperature of 25 °C. It depicts $\Delta c_{eq}(m)$ as a function of m. $\Delta c_{eq}(m)$ can be fitted by a quadratic expression. Therefore the second derivative becomes a constant $d^2\Delta c_{eq}/dm^2 = -0.3$ mol/m^3.

In the second scenario b) we assume a significantly higher P_{CO2}-value in the surface water, which may have been caused by organic CO_2-producing processes in the vadose zone. Therefore the P_{CO2} of the surface water is raised to P_{CO2} = 0.1 atm. $\Delta c_{eq}(m)$ also shown in Figure 3a, is no longer symmetric. In the region between m = 0.4 to m = 0.6 values are about –3 mol/m^3 one order of magnitude higher than in scenario a). It is just this region, where $\vec{\nabla}(m)^2$ exhibits its maximum. As a consequence porosity change is enhanced in scenario b) by one order of magnitude compared to scenario a). This will be discussed later in detail.

In scenario c) we assume that the water of the phreatic zone is in equilibrium with the $P_{CO2} = 3\ 10^{-4}$ atm of the atmosphere and the surface water now has a P_{CO2} of 0.05 atm. The second derivative has values of –2.17 mol/m^3 at m = 0.5. Also this scenario exhibits enhanced porosity change compared to scenario a). Fig. 3b shows the second derivative for the three scenarios.

To calculate the distribution $m(x,y)$ we use the modelling domain in Fig. 2. But, we now replace the two concentrations by their mixing ratios, $m = 1$ for the surface water and $m = 0$ for the phreatic water. The equation governing mixing m is Eq. 5, which we rewrite as

$$\Phi\frac{\partial m}{\partial t} = -q_y\frac{\partial m}{\partial y} + \Phi D\frac{\partial^2 m}{\partial x^2} + \Phi D\frac{\partial^2 m}{dy^2} \qquad (7)$$

To obtain the local distribution of m we create a numerical model using PMWIN (CHIANG & KINZELBACH, 2001). This software provides a front-end to MODFLOW (McDONALD & HARBAUGH, 1988) and MT3DMS (ZHENG & WANG, 1999). We use these models to calculate the distribution of m in our modelling domain (see Fig. 2).

3. RESULTS

We use the parameters $\Phi_0 = 0.3$, $v_y = 10^{-6}$ m/s and $d = 100\mu$m. Furthermore we assume a constant hydraulic conductivity in the entire modelling domain. Fig. 4 depicts the distribution of mixing m throughout the domain. As expected, the diffusion-mixing zone widens with distance from the entrance.
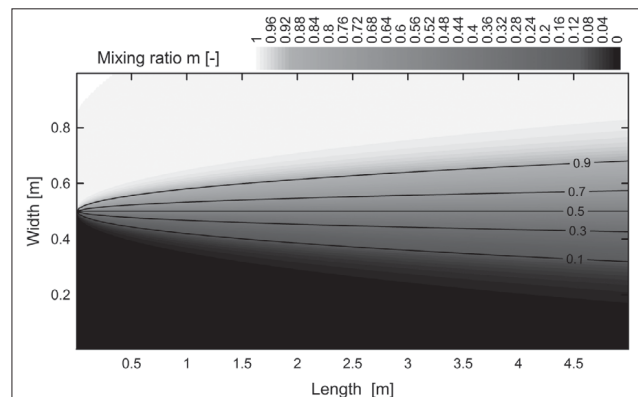

Figure 4: Spatial distribution of the mixing ratio m for a homogeneous aquifer in the modelling domain of Fig. 2. The curves give isolines of m. $v_y = 10^{-6}$ m/s.

By calculating numerically the partial derivatives $\partial m/\partial x$ and $\partial m/\partial y$ and applying Eq. 7 one obtains the initial change in porosity $d\Phi/dt_{/0}$ year^{-1}.

The increasing porosity causes a local positive feedback. From Eq. 7 we have

$$\frac{d\Phi(t)}{dt} = \frac{\Phi(t)}{\Phi_0}\, \frac{d\Phi}{dt_{/0}} \qquad (8)$$

and from this

$$\Phi(t) = \Phi_0 \exp\left(\frac{t}{\Phi_0 \cdot \tau}\right), \quad \frac{1}{\tau} = \frac{d\Phi}{dt_{/0}} \qquad (9)$$

Using the positive feedback of increasing porosity expressed in Eqs. 8 and 9, one can estimate an upper limit of the time T for the change of porosity from its initial value $\Phi_0 = 0.3$ to a value $V_0(T)=1$ as $T = -\Phi_0 \cdot \tau \cdot ln\,(\Phi_0)$. Therefore with $\Phi_0 = 0.3$ the maximum time T needed to excavate the region bordered by the isoline $1/\tau = d\Phi/dt_{/0}$ is about $T = 0.36 \cdot \tau$.

3.1. Geochemical scenario A: The inorganic case

In the following we will first discuss the results for the geochemical scenario a), where the second derivative is constant, because in this case the distribution of porosity change is proportional to $(\vec{\nabla}(m(x,y))^2$. Therefore all figures showing $d\Phi/dt_{/0}$ also reflect the local distribution of $(\vec{\nabla}(m(x,y))^2$. Fig. 5a illustrates the spatial distribution of porosity change by a gray scale. Furthermore it depicts isolines of $d\Phi/dt_{/0}$.

From Fig. 5 one visualizes that over a maximum time span of 120 000 years, a cave is created, extending to about 3 m in width and 0.2 in height. This is seen from the isoline with $3 \cdot 10^{-6}$ year^{-1}. To excavate a void of about 1m width and 0.1 in height (isoline $1 \cdot 10^{-5}$ year^{-1}), only 38 000 years are needed. These numbers are the upper limits because porosity changes increase inside the region bordered by the isoline. Fig. 5b illustrates the distribution of initial change of porosity along transects in the x-direction with $y = 0.1, 0.5, 1$ and 2.5 m. Porosity change decreases with increasing distance from the input in the y-direction, such that evolution of porosity is restricted to a region extending a few metres away from the input in the flow direction. In the transverse direction to flow along x this region is limited to several tenths of a metre.

Flow velocities in the Floridan aquifer are as low as several 10^{-7} m/s. Therefore in Fig. 6 we show the results for a flow velocity of $5 \cdot 10^{-7}$ m/s, everything else being unchanged in comparison to Fig. 5. Due to the low flow velocities, the region where the diffusion-mixing zone exhibits high gradi-
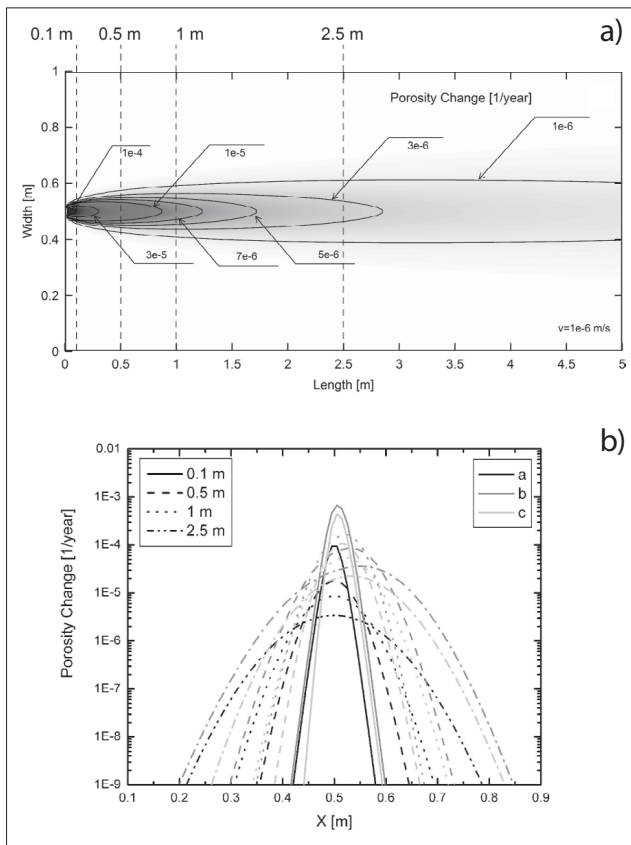

Figure 5: a) Spatial distribution of initial porosity change $d\Phi/dt_{/0}$. The isolines represent porosity change in year^{-1} for the geochemical scenario a (inorganic). $v_y = 10^{-6}$ m/s; b) Vertical distribution of initial porosity change for the three geochemical scenarios a, b, and c along transects shown in panel *a* as vertical lines.

Figure 6: a) Spatial distribution of initial porosity change $d\Phi/dt_{/0}$. The isolines represent porosity change in year^{-1} a) the geochemical scenario a (inorganic). $v_y = 5 \cdot 10^{-7}$ m/s; b) Vertical distribution of initial porosity change for the three geochemical scenarios a, b, and c along transects shown in panel *a* as vertical lines.
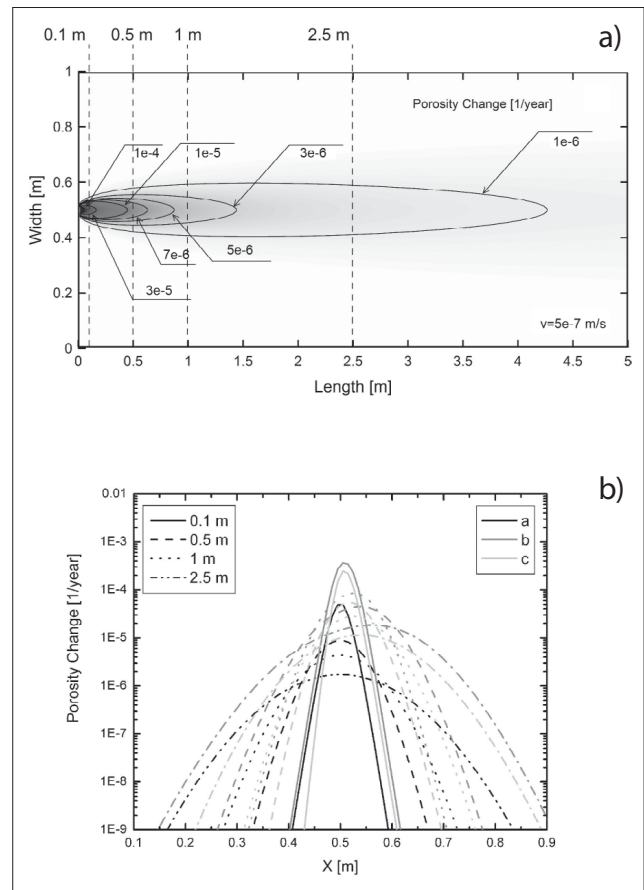
ents and consequently high changes of porosity, becomes smaller as can be seen by the isoline of $3 \cdot 10^{-6}$ year^{-1}. The cavity created in 120 000 years extends only to 1m from the input in the y – direction and has a height of about 0.1m. The distribution of porosity change in the x – direction along the transect in Fig. 6b closely resembles that of Fig. 5b, but the porosity change is lower in the centre of the diffusion-mixing zone.

3.2. Geochemical scenarios b) and c): The organic case

The times of cave evolution in the inorganic scenario are too long to explain the existence of isolated caves in Florida. These have originated during Quaternary sea level changes, where times of constant sea level elevations lasted no longer than 10 000 years. MYLROYE & MYLROYE (2007) have suggested that biogenic decay of organic matter caught on the top of the phreatic mound of the surface water increases its CO_2 concentration. We have taken this into account by increasing the P_{CO2} of the surface waters in the geochemical scenarios b) and c). As can be seen in Fig. 3b the second derivatives are higher by almost a factor of ten for $m \approx 0.5$. Therefore one expects the evolution of caves in time scales of 10 000 years, supporting Mylroye's thesis.

We have modelled these organic cases. Transects of the evolution of porosity in comparison to the inorganic scenario are illustrated in Figs. 5b and 6b. They show that porosity changes are indeed significantly higher for both organic scenarios. Due to the asymmetry of the second derivatives the maximum of porosity evolution shifts upwards into the surface water region. These results indicate that caves with dimensions of about 1m width and 0.2 m in height can be created along the border where surface water with higher P_{CO2} encounters the water table of the phreatic base flow. This way we obtain blind ending passages of several 10 m to 100 m length. These results are in concordance with the height to width ratios observed by FLOREA (2006) in the caves of West Central Florida. Most of them (47%) have ratios of about 0.3, similar to our values of about 0.1. The time needed to create such caves is in the order of 10 000 years. Note that our modelling assumes a constant sea level during the entire time of evolution to which the palaeo water table of the phreatic aquifer was tied. It should be noted here that at present in this work we have only modelled initial porosity changes and have just considered the feedback by Eqs. 8–11 to estimate an upper limit of the time for cave evolution. Future modelling should take into account changes of hydraulic conductivity due to the change in porosity. The corresponding changes in the flow pattern by focusing of flow lines and the corresponding increase in mixing gradients might enhance porosity change in time.

Our modelling results show that due to the rise of P_{CO2} – levels by decomposition of organic matter in the water seeping down to the phreatic aquifer significant voids and caves similar to those observed in Florida can originate in a time scale of 10 000 years as an upper limit. These are the maximum times of constant sea level stand in the Quaternary.

For the inorganic scenario, significant changes of porosity from 0.3 to 0.5 arise within time spans of about 10 000 years in regions with $d\Phi/dt_{/0} = 10^{-5}$ year^{-1}. In the organic scenarios, even if the times of constant boundary conditions are too short for the evolution of caves, changes in porosity by about 50 % need time spans of about 1000 years.

4. CONCLUSION

When two carbonate waters saturated with respect to calcite, but with different concentrations of calcium meet in an aquifer, they are mixed, and the spatial distribution of the mixing ratio $m(x,y)$ describes the degree of mixing. Depending on m an amount $\Delta c_{eq}(m)$ is dissolved in the diffusion-mixing zone by mixing corrosion and the porosity of the rock increases. The change $d\Phi/dt$ in porosity depends critically on the spatial distribution of $m(x,y)$ and on the chemistry of the mixed solution. When the two water bodies meet along a one dimensional border, isolated caves with blind ending passages can develop in the diffusion-mixing zone extending along such boundary lines. As long as these are located in the phreatic zone, flow through them is directed transverse to these passages and horizontally along the water table.

We have modelled cave evolution for a hydrogeological scenario where surface water with elevated P_{CO2} of 0.1 atm, originating from biogenic decay of organic matter, enters the water table of an unconfined aquifer below. The results of these modelling attempts closely resemble caves in West – Central Florida (FLOREA, 2006; FLOREA et al., 2007).

This concept of horizontal transverse speleogenesis could be used in the future to explain the evolution of isolated caves, in other karst areas, such as those described at Mt Scopus Formation (Israel) by FRUMKIN & FISCHHENDLER (2005). Our concept should not be mixed with the concept of hypogenic ascending speleogenesis by KLIMCHOUK (2007). In this case, aggressive water ascends from adjacent formations below the cave level through fractures, and flow crosses the cave passages vertically. The modelling approach presented here is a first step into gaining an understanding of speleogenesis of isolated caves in porous rock, which are so much different from the caves arising by dissolution of limestone with negligible porosity by aggressive solutions flowing along fractures from an input to an output.

REFERENCES

CHIANG, W.H. & KINZELBACH, W. (2001): 3D-Groundwater Modeling with PMWIN.– Springer-Verlag, Berlin, Heidelberg, New York, 397 p.

DAVIS, H. (1996): Hydrogeologic investigation and simulation of groundwater flow in the Upper Floridan aquifer of north-central Florida and southwestern Georgia and delineation of contributing areas for selected City of Tallahassee, Florida, water-supply wells: U.S. Geological Survey Water-Resources Investigations Report, 95–4296.

DREYBRODT, W. (1988): Processes in Karst Systems.– Physics, Chemistry, and Geology, Springer, Berlin, 288 p.

DREYBRODT, W. & GABROVŠEK, F. (2003): Basic processes and mechanisms governing the evolution of karst. / Speleogenesis and

Evolution of Karst Aquifers 1 (1), re-published from: GABROVŠEK, F. (ed.): Evolution of karst: from prekarst to cessation. Postojna–Ljubljana: Zalozba ZRC, 115–154.

DREYBRODT, W. & ROMANOV, D. (2007): Time scales in the evolution of solution porosity in porous coastal carbonate aquifers by mixing corrosion in the saltwater – freshwater transition zone.– Acta Carsologica, 36/1, 25–34.

DREYBRODT, W., GABROVŠEK, F. & ROMANOV, D. (2005): Processes of speleogenesis: A modeling approach.– Karst Research Institute, ZRC SAZU, Postojna, Slovenia.

FLOREA, L.J. (2006): Architecture of air-filled caves within the karst of the Brooksville Ridge, west-central Florida.– Journal of Cave and Karst Studies, 68/2, 64–75.

FLOREA, L.J., VACHER, H.L., DONAHUE, B. & NAAR, D. (2007): Quaternary cave levels in peninsular Florida.– Quaternary Science Reviews, 26, 1344–1361.

FLOREA, L.J. & VACHER, L.H. (2004): Cave levels, marine terraces, paleoshorelines, and the water table in peninsular Florida.– Archives of climate change in karst. Karst Waters Institute Special Publication, 10.

FORD, D.C. & WILLIAMS, P.W. (2007): Karst Hydrogeology and Geomorphology.– John Wiley & Sons Ltd., 562 p.

FRUMKIN, A. & FISCHHENDLER, I. (2005): Morphometry and distribution of isolated caves as a guide for phreatic and confined paleohydrological conditions.– Geomorphology, 67, 457–471.

HANSHAW, B.B., BACK, B. & RUBIN, M. (1965): Radiocarbon Determinations for Estimating Groundwater Flow Velocities in Central Florida.– Science, 23, 494–495, doi: 10.1126/science.148.3669.494.

KAUFMANN, G. (2005): Structure and evolution of karst aquifers: a finite-element numerical modeling approach.– In: DREYBRODT, W., GABROVŠEK, F. & ROMANOV, D. (eds.): Processes of Speleogenesis: A modeling approach. Karst Research Institute, ZRC SAZU, Postojna, Slovenia, 323–371.

KLIMCHOUK, A. (2007): Hypogene Speleogenesis: Hydrological and Morphogenetic Perspective, National Cave and Karst Research Institute. Special Paper No.1.

McDONALD, M.C. & HARBAUGH, A.W. (1988): MODFLOW, A modular three – dimensional finite difference ground – water flow model.– U. S. Geological Survey, Open – file report, 83–875.

MOTZ, L.H. (1998): Vertical leakage and vertically averaged vertical conductance for karst lakes in Florida.– Water Resources Research, 34, 159–167.

MOTZ, L.H., SOUSA, G.D. & ANNABLE, M.D. (2001): Water budget and vertical conductance for Lowry (Sand Hill) Lake in north central Florida, USA.– Journal of Hydrology, 250, 134–148.

MYLROIE, J.E. & CAREW, J.L. (1990): The flank margin model for dissolution cave development in carbonate platforms. Earth Surface Processes and Landforms, 15, 413–424.

MYLROIE, J.E. & CAREW, J.L. (2000): Speleogenesis in coastal and oceanic settings.– In: KLIMCHOUK, A., FORD, D.C., PALMER, A. & DREYBRODT, W. (eds.): Speleogenesis: Evolution of Karst Aquifers. National Speleological Society, Huntsville, 226–233.

MYLROIE, J.E. & CAREW, J.L. (2003): Karst development on carbonate islands. Speleogenesis and Evolution of Karst Aquife & HARRIS, P.A. (eds.), 1995. Unconformities in Carbonate Strata – Their Recognition and the Significance of Associated Porosity, AAPG Memoir, 63, 55–76.

MYLROIE, J.E. & MYLROIE, J.R. (2007): Development of the Carbonate Karst Model.– Journal of Cave and Karst Studies, 69, 59–75.

PALMER, A.N. (1991): Origin and morphology of limestone caves.– Geological Society of America BULLETIN, 103/1, 1–21.

PALMER, A.N. (2007): Cave Geology.– Cave Books, 454 p.

PARKHURST, D.L. & APPELO, C.A.J. (1999): User's guide to PHREE-QC (version 2). A computer program for speciation, batch-reaction, one-dimensional transport, and inverse geochemical calculations: U.S. Geological Survey Water-Resources Investigations Report 99–4259, 312 p.

PHILLIPS, O.M. (1991): Flow and Reactions in Permeable Rocks.– Cambridge University Press, New York, 285 p.

ROMANOV, D. & DREYBRODT, W. (2006): Evolution of porosity in the saltwater-freshwater diffusion-mixing zone of coastal carbonate aquifers: An alternative modeling approach.– Journal of Hydrology, 329, 661–673.

WERTH, C.J., CIRPKA, O.A. & GRATHWOHL, P. (2005): Enhanced mixing and reaction through flow focusing in heterogeneous porous media Water Resour. Res., 42, 12, W12414 10.1029/2005WR 004511

ZHENG, C. & WANG, P.P. (1999): MT3DMS, A modular three-dimensional multi-species transport model for simulation of advection, dispersion and chemical reactions of contaminants in groundwater systems; documentation and user's guide, U.S. Army Engineer Research and Development Center Contract Report SERDP-99-1, Vicksburg, MS, 202 p.